Centrum voor Wiskunde en Informatica

REPORT*RAPPORT*

MAS

Modelling, Analysis and Simulation

Modelling, Analysis and Simulation

High-Order TVD and TVB Linear Multistep Methods

S.J. Ruuth, W. Hundsdorfer

CWI is the National Research Institute for Mathematics and Computer Science. It is sponsored by the Netherlands Organization for Scientific Research (NWO).
CWI is a founding member of ERCIM, the European Research Consortium for Informatics and Mathematics.

CWI's research has a theme-oriented structure and is grouped into four clusters. Listed below are the names of the clusters and in parentheses their acronyms.

Probability, Networks and Algorithms (PNA)

Software Engineering (SEN)

Modelling, Analysis and Simulation (MAS)

Information Systems (INS)

High-Order TVD and TVB Linear Multistep Methods

ABSTRACT

We consider linear multistep methods that possess the TVD (total variation diminishing) or TVB (total variation bounded) properties, or related general monotonicity and boundedness properties. Strict monotonicity or TVD, in terms of arbitrary starting values for the multistep schemes, is only valid for a small class of methods, under very stringent step size restrictions. This makes them uncompetitive to the TVD Runge-Kutta methods. By relaxing these strict monotonicity requirements a larger class of methods can be considered, including many methods of practical interest. In this paper we construct linear multistep methods of high-order (up to six) that possess relaxed monotonicity or boundedness properties with optimal step size conditions. Numerical experiments show that the new schemes perform much better than the classical TVD multistep schemes. Moreover there is a substantial gain in efficiency compared to recently constructed TVD Runge-Kutta methods.

HIGH-ORDER TVD AND TVB LINEAR MULTISTEP METHODS

STEVEN J. RUUTH [*] AND WILLEM HUNDSDORFER [†]

Abstract. We consider linear multistep methods that possess the TVD (total variation diminishing) or TVB (total variation bounded) properties, or related general monotonicity and boundedness properties. Strict monotonicity or TVD, in terms of arbitrary starting values for the multistep schemes, is only valid for a small class of methods, under very stringent step size restrictions. This makes them uncompetitive to the TVD Runge-Kutta methods. By relaxing these strict monotonicity requirements a larger class of methods can be considered, including many methods of practical interest.

In this paper we construct linear multistep methods of high-order (up to six) that possess relaxed monotonicity or boundedness properties with optimal step size conditions. Numerical experiments show that the new schemes perform much better than the classical TVD multistep schemes. Moreover there is a substantial gain in efficiency compared to recently constructed TVD Runge-Kutta methods.

Key words. Multistep schemes, monotonicity, TVD, TVB, SSP, strong stability

AMS subject classifications. 65L06, 65M06, 65M20

1. Introduction. Apart from the usual linear stability and consistency requirements, nonlinear monotonicity and boundedness properties are often essential for numerical schemes to approximate non-smooth solutions in a qualitatively correct manner. In this paper we shall be concerned with systems of ordinary differential equations (ODEs) in $\mathbb{R}^m$,

$$(1.1) \qquad w'(t) = F(w(t)), \quad w(0) = w_0.$$

In our applications, the ODE systems will arise from semi-discretization of (hyperbolic) partial differential equations (PDEs). Specifically we are interested in the discrete preservation of monotonicity and boundedness properties by numerical approximations $w_n \approx w(t_n)$, $t_n = n\Delta t$, generated by linear multistep methods.

In the following we assume that there is a maximal step size $\Delta t_{FE} > 0$ such that

$$(1.2) \qquad \|v + \Delta t\, F(v)\| \leq \|v\| \qquad \text{for all } 0 < \Delta t \leq \Delta t_{FE},\ v \in \mathbb{R}^m,$$

where $\|\cdot\|$ is a given semi-norm, such as the total variation over the components. Of course, with the forward Euler method this leads to

$$(1.3) \qquad \|w_n\| \leq \|w_0\| \qquad \text{for all } n \geq 1,$$

whenever the step size restriction $\Delta t \leq \Delta t_{FE}$ is valid. Similar properties will be examined for higher-order methods.

We shall mainly consider explicit linear multistep methods

$$(1.4) \qquad w_n = \sum_{j=1}^{k} \left(a_j w_{n-j} + b_j \Delta t F(w_{n-j}) \right), \qquad n \geq k,$$

[*]Department of Mathematics, Simon Fraser University, Burnaby, British Columbia, V5A 1S6 Canada (`sruuth@sfu.ca`). The work of this author was partially supported by a grant from NSERC Canada.

[†]CWI, P.O. Box 94079, 1090 GB Amsterdam, The Netherlands (`willem.hundsdorfer@cwi.nl`).

where the starting vectors $w_0, w_1, \cdots, w_{k-1}$ are either given or computed by an appropriate starting procedure. A common generalization of (1.3) for multistep methods is

$$(1.5) \qquad \|w_n\| \ \leq \ \max_{0 \leq j \leq k-1} \|w_j\| \,.$$

However, this property is only valid for a small class of methods under stringent step size restrictions; see § 2 for a brief review.

It was shown in [6] that methods of practical relevance can be included in the theory if we consider multistep methods in combination with starting procedures that generate $w_1, w_2, \ldots, w_{k-1}$ from w_0. Instead of (1.5) we will consider the property

$$(1.6) \qquad \|w_n\| \ \leq \ M \, \|w_0\| \quad \text{for all} \ \ n \geq 1 \,,$$

where the size of the constant $M \geq 1$ will be determined by the starting procedure. In case $M = 1$, this will be referred to as *monotonicity*. If $M \geq 1$ this is a boundedness property. Following [6] we can determine constants C_{LM} such that (1.6) holds under the step size restriction $\Delta t \leq C_{LM} \Delta t_{FE}$.

Example 1.1. The main application of such monotonicity and boundedness results are found in the numerical solution of hyperbolic PDEs, in particular for conservation laws. Let us consider as an example the one-dimensional equation

$$(1.7) \qquad u_t + f(u)_x = 0 \,.$$

Spatial discretization will lead to a system of ODEs where the components of $w(t)$ approximate the PDE solution at grid points or surrounding cells, $w_j(t) \approx u(x_j, t)$. The discrete total variation $\|v\| = \mathrm{TV}(v)$ is a semi-norm defined as

$$\mathrm{TV}(v) = \sum_j |v_j - v_{j-1}| \,,$$

where e.g. $v_0 = v_m$ for problems with periodic boundary conditions. For this semi-norm, the property (1.2) is called the TVD (total variation diminishing) property, and its generalization (1.6) with $M \geq 1$ is called the TVB (total variation bounded) property. Conservative schemes with this boundedness property are known to converge to the correct entropy solutions for hyperbolic conservation laws; see for instance [3] for details. Finally we note that for hyperbolic problems the step size restriction $\Delta t \leq C_{LM} \Delta t_{FE}$ is often called a CFL condition and the threshold C_{LM} is then the CFL coefficient. $\square$

In [6] property (1.6) and the step size restriction $\Delta t \leq C_{LM} \Delta t_{FE}$ was studied for several well-known schemes, in particular explicit Adams and extrapolated BDF schemes. In this paper, high-order methods will be constructed that satisfy the boundedness property (1.6) with optimal threshold factors C_{LM}.

Numerical tests on some scalar conservation laws will show that our new optimal multistep methods are superior to the optimal schemes of [2, 13, 18] that satisfy (1.5). In these experiments also monotone (TVD, SSP) Runge-Kutta methods of [9, 15, 19, 20] will be taken into consideration, and also these methods will be seen to be less efficient in the tests than our new multistep schemes.

In § 2 a brief review is presented of multistep methods satisfying (1.5), including some (minor) improvements on the methods listed in [2]. The main section of this paper is § 3, where optimal methods satisfying (1.6) with order $p = 3, 4, 5, 6$ and step number $k = p$ or $k = p + 1$ will be constructed. Numerical illustrations are given in § 4. The final § 5 contains a summary and conclusions.

2. Monotonicity and TVD with Arbitrary Starting Values.

2.1. Methods with Non-negative Coefficients. Assume that all $a_j, b_j \geq 0$. By regarding the step (1.4) as a linear combination of scaled forward Euler steps it easily follows that the monotonicity property (1.5) will be valid under (1.2) with the step size restriction

$$(2.1) \qquad \Delta t \ \leq \ K_{LM} \, \Delta t_{FE} \,, \qquad K_{LM} = \min_{1 \leq j \leq k} \frac{a_j}{b_j} \qquad \text{if } a_j, b_j \geq 0 \text{ for all } j \,,$$

with convention $0/0 = +\infty$. This result is due to Shu [18], where it was formulated with total variations. For explicit methods with $k \geq 2$, Lenferink [13] showed that

$$(2.2) \qquad K_{LM} \ \leq \ \frac{k-p}{k-1} \,.$$

Hence $K_{LM} > 0$ is not possible for any method with $p = k$.

The optimal schemes of order 2 are given by [13, 18]

$$(2.3) \qquad a_1 \ = \ \frac{k(k-2)}{(k-1)^2} \,, \quad a_k \ = \ \frac{1}{(k-1)^2} \,, \quad b_1 \ = \ \frac{k}{k-1} \,,$$

with the other coefficients zero. Higher-order schemes have been constructed in [13, 18], mainly numerically. Our preferred technique is based on a recent approach of [17] for optimizing TVD Runge-Kutta methods. Since we shall use this technique below for deriving new schemes, we describe it here in some detail.

We begin by noting that optimal k-step schemes of order p can be derived by maximizing K_{LM}. Here, the order conditions give $p + 1$ relations for the coefficients a_j, b_j [4, 10]. However, this formulation of the nonlinear programming (NLP) problem does not lend itself easily to numerical solution; see [20] for further discussion. By introducing a dummy variable z, the nonlinear programming problem can be reformulated as finding

$$(2.4a) \qquad \max_{(a_j, b_j)} z \,,$$

subject to the $p + 1$ order conditions and

$$(2.4b) \qquad a_i \,, \ b_i \ \geq \ 0 \,, \qquad i = 1, 2, \ldots, k \,,$$
$$(2.4c) \qquad a_i - z b_i \ \geq \ 0 \,, \qquad i = 1, 2, \ldots, k \,.$$

This NLP formulation is comprised of factorable objective and constraint functions and thus is suitable for optimization in BARON [1], which is a commercially-available, deterministic global branch-and-bound optimization program.

To guarantee optimality in BARON we typically need to supply bounds to all the variables. Fortunately we know that all the a_i are bounded by 1 (because $\sum_i a_i = 1$) and all the b_i are bounded by the inverse of K_{LM}. Finding globally optimal schemes and guaranteeing their optimality is surprisingly efficient. For example, BARON 5.0 finds the optimal fifty-step, fourth-order scheme and guarantees its optimality in just 0.58 seconds on a 1.2 GHz Athlon machine.

A list of guaranteed globally optimal schemes for k up to six with order p equal to three or four is given in Table A.1 at the end of this paper. Because the coefficients of the schemes are all non-negative, we refer to the optimal k-step, order-p TVD linear multistep scheme as $\text{TVD}_+(k, p)$.

Fifth- and sixth-order TVD multistep schemes require at least seven steps and do not appear in the table. In view of (2.2), all methods in the table have $k > p$.

The optimal third-order $\text{TVD}_+(4,3)$, $\text{TVD}_+(5,3)$ [18, 13] and $\text{TVD}_+(6,3)$ [13] schemes have been known for some time and we reproduce them here for convenience. The remaining $\text{TVD}_+(5,4)$ and $\text{TVD}_+(6,4)$ schemes have K_{LM} values that agree with the bounds provided in [13].

2.2. Schemes with Spatial Downwinding. As noted in [18], the assumption $b_j \geq 0$ can be avoided for discretizations of conservation laws (1.7). If $b_j < 0$, then $F(w_{n-j})$ in (1.4) should be replaced by $\tilde{F}(w_{n-j})$, where $w' = -\tilde{F}(w)$ is the semi-discretization of the equation with reversed time $u_t - f(u)_x = 0$. Its realization in practice is simply a reversal of the upwind direction in the spatial discretization. Instead of (2.1) this modification will give the step size restriction

$$(2.5) \qquad \Delta t \ \leq \ \tilde{K}_{LM} \, \Delta t_{FE} \,, \qquad \tilde{K}_{LM} = \min_{1 \leq j \leq k} \frac{a_j}{|b_j|} \quad \text{if } a_j \geq 0 \text{ for all } j$$

to achieve (1.5).

The following result gives an upper bound for this threshold factor for second-order schemes. The proof is given in Appendix B.

THEOREM 2.1. *For second-order k-step methods we have $\tilde{K}_{LM} \leq (k-1)/k$. This upper bound is achieved for $k \geq 2$ by the schemes (1.4) with*

$$a_1 = \frac{k^2}{k^2+1}, \quad a_k = \frac{1}{k^2+1}, \quad b_1 = \frac{k^3}{(k-1)(k^2+1)}, \quad b_k = -\frac{k}{(k-1)(k^2+1)} \,,$$

and all other coefficients equal to zero.

Higher-order schemes have been constructed numerically in [18]. We derive globally optimal schemes with downwinding by extending our optimizations for non-negative coefficient schemes.

Following [17], we introduce a dummy variable z and we write $b_i = \sigma_i \tilde{b}_i$ with $\tilde{b}_i = |b_i|$ and $\sigma_i = \text{sgn}(b_i) = \pm 1$. Then the optimization becomes

$$(2.6a) \qquad \max_{(a_j, \tilde{b}_j, \sigma_j)} z \,,$$

subject to the $p + 1$ order conditions and the constraints

$$(2.6b) \qquad a_i \,, \ \tilde{b}_i \ \geq \ 0 \,, \quad i = 1, 2, \ldots, k \,,$$
$$(2.6c) \qquad a_i - z\tilde{b}_i \ \geq \ 0 \,, \quad i = 1, 2, \ldots, k \,.$$

Notice that this mixed integer nonlinear programming formulation is comprised of factorable objective and constraint functions and that the variables are easily bounded. Thus this is a suitable mathematical formulation for finding guaranteed optimal solutions in BARON. However, the total computational effort can be reduced substantially by instead solving 2^k NLP problems, each corresponding to one of the possible sign combinations. This leads to a total of 2^k cases each of which only requires a fraction of a second to solve in BARON 5.0.

Using this approach, a list of guaranteed globally optimal schemes was constructed for orders $p = 3, 4, 5, 6$ and $k \leq 6$. This is presented in Table A.2 at the end of this paper. Following the convention described in the previous section, we denote the optimal k-step, order-p scheme with $a_j \geq 0$ and unrestricted coefficients b_j as $\text{TVD}_\pm(k, p)$.

The schemes $\text{TVD}_\pm(4,3)$, $\text{TVD}_\pm(5,3)$, $\text{TVD}_\pm(5,4)$, and $\text{TVD}_\pm(6,6)$ are new. Our study for the optimal six-step, third-order scheme is also new; however, there the non-negative coefficient scheme $\text{TVD}_+(6,3)$, first presented in [13], is optimal. The optimal schemes $\text{TVD}_\pm(3,3)$, $\text{TVD}_\pm(4,4)$ presented in Table A.2 essentially agree with earlier schemes from Gottlieb, Shu and Tadmor [2]. Some improvements were found in the remaining three cases over earlier studies [18, 2]. Specifically, 16%, 12% and 1% improvements in $\tilde{K}_{LM}$ were found for $\text{TVD}_\pm(6,4)$, $\text{TVD}_\pm(5,5)$, and $\text{TVD}_\pm(6,5)$, respectively.

Comparing the $\text{TVD}_\pm(k,p)$ and the $\text{TVD}_+(k,p)$ schemes, it should be noted that for the $\text{TVD}_\pm(k,p)$ schemes both function evaluations F_n and $\tilde{F}_n$ will be needed. If more than one processor is available, these evaluations can be carried out in parallel. On a serial machine, however, these schemes will be approximately two times more expensive per step. Moreover, the use of downwind discretizations may add some numerical diffusion that will persist even for small step sizes; see the test results in § 4.

3. Boundedness and TVB for Higher-Order Methods. The above monotone multistep schemes are not competitive with the Runge-Kutta schemes of [9, 15, 20]. However, by considering the multistep schemes in combination with starting procedures, it is possible to consider schemes that satisfy the boundedness property (1.6) with a constant M whose size is determined by the starting procedure [6].

This section contains derivations of optimal boundedness results for explicit linear multistep methods of order $p = 3, 4, 5, 6$. To study the boundedness property (1.6), with $M \geq 1$, it is not necessary to specify the starting schemes: while the value of M may vary according to the starting procedure, the boundedness property itself is independent of the chosen startup.

3.1. Reformulations. The derivation of boundedness results is largely based on suitable reformulations of the schemes, whereby a k-step scheme is first rewritten as an equivalent $(k + 1)$-step scheme with a free parameter, then as a $(k + 2)$-step scheme with two free parameters, etc., up to the starting values. The free parameters can then be selected such that the scheme has non-negative coefficients.

To keep the presentation concise and clear, we give such reformulation here in detail only for three-step schemes; the general formulas can be found in [5]. Consider (1.4) with $k = 3$. Then by subtracting and adding $\theta_1 \ldots \theta_j w_{n-j}$, $j = 1, 2, \ldots, n - 3$, substituting w_{n-j} in terms of w_{n-j-i}, $i = 1, 2, 3$, and collecting terms, it follows that w_n can be expressed as

$$(3.1) \qquad w_n = \sum_{j=1}^{n-3} \left(\alpha_j w_{n-j} + \beta_j \Delta t F_{n-j} \right) + \sum_{i=0}^{2} \left(\alpha_{n,n-i}^R w_i + \beta_{n,n-i}^R \Delta t F_i \right),$$

where the coefficients α_j, β_j are given by

$$\alpha_1 = a_1 - \theta_1, \quad \alpha_2 = a_2 + a_1 \theta_1 - \theta_1 \theta_2, \quad \alpha_3 = a_3 + a_2 \theta_1 + a_1 \theta_1 \theta_2 - \theta_1 \theta_2 \theta_3,$$

$$\alpha_j = \left(\prod_{k=1}^{j-3} \theta_k \right) \left(a_3 + a_2 \theta_{j-2} + a_1 \theta_{j-2} \theta_{j-1} - \theta_{j-2} \theta_{j-1} \theta_j \right), \quad j \geq 4,$$

$$\beta_1 = b_1, \quad \beta_2 = b_2 + b_1 \theta_1, \quad \beta_3 = b_3 + b_2 \theta_1 + b_1 \theta_1 \theta_2,$$

$$\beta_j = \left(\prod_{k=1}^{j-3} \theta_k \right) \left(b_3 + b_2 \theta_{j-2} + b_1 \theta_{j-2} \theta_{j-1} \right), \quad j \geq 4.$$

For k-step methods with $k \geq 4$ we can proceed similarly. In the above reformulation (3.1) we get the same expressions for α_1, α_2, α_3 and β_1, β_2, β_3; the other α_j, β_j will then involve more terms.

We shall take $\theta_i \geq 0$ such that

$$(3.2) \qquad\qquad \alpha_j \geq 0, \quad \beta_j \geq 0 \qquad \text{for all } j \geq 1,$$

and we define

$$(3.3) \qquad\qquad C_{LM} = \max_{\{\theta_i\}_{i \geq 1}} \min_{j \geq 1} \frac{\alpha_j}{\beta_j}.$$

In the search for favourable schemes we will require that $\theta_j = \theta_* < 1$ for all $j \geq j_*$; see also [5] for some comments on this. Under these assumptions it follows that the boundedness property (1.6) holds with $M \geq 1$ for step sizes $\Delta t \leq C_{LM}\Delta t_{FE}$. To obtain results for genuine monotonicity, that is, $M = 1$, it is also necessary to study the coefficients $\alpha^R_{n,n-i}$ and $\beta^R_{n,n-i}$ of the remainder term in (3.1) and to include specific starting procedures. For a detailed analysis, we refer to [6] for the case $k = 2$ and to [5] for $k \geq 3$.

3.2. Optimizations of C_{LM}. Two-step, second order explicit methods can be studied by hand, as it was done in [6]. Methods involving more steps are more involved, and naturally lead us to consider numerical optimization techniques. Following § 2.1, we formulate the optimization problem by introducing a dummy variable z that corresponds to C_{LM}; however, now all the α_i, β_i must be constrained to be non-negative. We have carried out extensive optimizations in BARON to determine numerically optimal schemes. A guarantee of optimality is not sought since the overall complexity of the optimization problem makes this much more difficult.

The schemes that are found this way for given step number k and order p will be denoted as $\text{TVB}(k, p)$. Somewhat surprisingly, seeking optimal schemes often led to a value $\theta_* = 0$. This means that all coefficients α_j, β_j are zero for $j \geq k + j_*$, and hence the reformulation then gives a l-step scheme, $l = k + j_* - 1$, with non-negative coefficients. This extended scheme is reducible to the original k-step method [4], so it should primarily be regarded for theoretical interest. Schemes with $\theta_* = 0$ will be denoted by $\text{TVB}_0(k, p)$. Finally we note that for all the new schemes presented in this section the error constants turned out to be of moderate size.

3.3. An Order-Three Scheme. We first optimize C_{LM} over the class of three-step, third-order linear multistep schemes with fifteen θ-values. This yields a scheme that satisfies the boundedness property (1.6) with $M \geq 1$ provided $\Delta t \leq 0.537\Delta t_{FE}$. The coefficients are given in Table 3.3. It is noteworthy that the optimization leads to $\theta_{10} = 0$, implying this scheme can be rewritten as a twelve-step scheme that is TVD with arbitrary starting values. Because of this property, we will refer to this scheme as $\text{TVB}_0(3,3)$.

It is interesting to compare this $\text{TVB}_0(3,3)$ scheme against the third-order extrapolated BDF scheme (eBDF3)

$$(3.4) \quad w_n = \frac{18}{11}w_{n-1} - \frac{9}{11}w_{n-2} + \frac{2}{11}w_{n-3} + \frac{18}{11}\Delta t F_{n-1} - \frac{18}{11}\Delta t F_{n-2} + \frac{6}{11}\Delta t F_{n-3},$$

which is the best reported third-order scheme in [6]. Because its threshold value is given by $C_{LM} = 7/18$, the new scheme $\text{TVB}_0(3,3)$ gives a 38% improvement over eBDF3 in allowable (stable) step size, for which (1.6) is ensured.

The new $\text{TVB}_0(3,3)$ scheme also has a relatively large linear stability region, showing where linear stability is valid for the scalar, complex test equation $w' = \lambda w$, $z = \Delta t\, \lambda$. The $\text{TVB}_0(3,3)$ stability region includes a part of the imaginary axis. See Figure 3.1 for a comparison of the stability region of this scheme and the eBDF3 scheme.

Although the form of the stability regions is not directly related to monotonicity properties, it seems that for higher-order spatial discretizations violation of the linear (von Neumann) stability conditions often leads to inaccurate solutions due to numerical *compression* of smooth solutions; see for instance [7, Sect. 1.3] for an illustration. Having a portion of the imaginary axis and some region to the left of it in the stability region ensures that the scheme will be stable under appropriate CFL restriction in the classical, linear sense for any spatial discretization.

TABLE 3.1

The coefficients of the numerically optimal three-step, third-order linear multistep scheme.

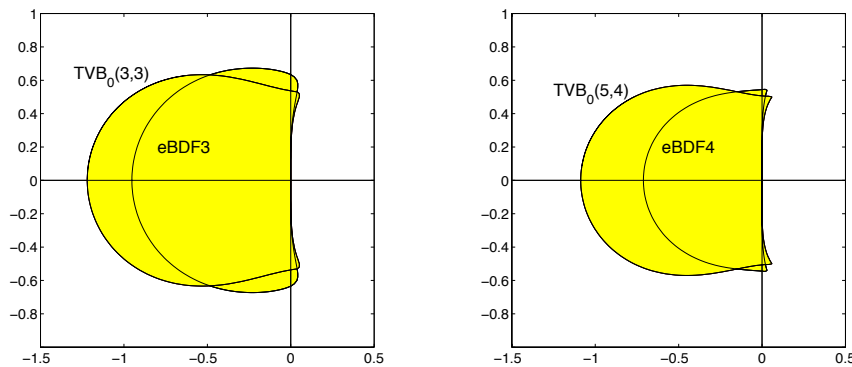| $\text{TVB}_0(3,3)$	a_i	b_i	C_{LM}
$i = 1$	1.908535476882378	1.502575553858997	0.537252303224424
$i = 2$	-1.334951446162515	-1.654746338401493	
$i = 3$	0.426415969280137	0.670051276940255	

FIG. 3.1. *Stability regions for the eBDF3 and $\text{TVB}_0(3,3)$ schemes (left plot) and the eBDF4 and $\text{TVB}_0(5,4)$ schemes (right plot). The $\text{TVB}(4,4)$ region is not shown since it closely agrees with the $\text{TVB}_0(5,4)$ region.*

3.4. Fourth-Order Schemes.

3.4.1. Four-Step Schemes. We direct our attention next to the class of four-step, fourth-order linear multistep methods. In the reformulations for this class, we were unable to find schemes which allowed arbitrary starting values in an extended version (i.e., $\theta_* = 0$). Moreover, taking $\theta_j = \theta_*$ for all $j \geq j_*$ we found that C_{LM} increases as $\theta_* \in [0, 1)$ increases. Unfortunately the choice $\theta_* = 1$ does not lead to a scheme that is stable; the scheme turned out to have two characteristic roots equal to one, giving weak instability. For θ_* close to 1, the (scaled) error constants [4, p. 373] are large. Selecting an appropriate scheme is therefore quite interesting and subtle, since larger θ_*-values give larger C_{LM}-values while smaller θ_*-values give better accuracy and also seem to minimize the possibility of oscillations arising from the startup procedures when $M > 1$.

On the balance, we bias our choice towards large time steps by taking $\theta_* = 0.7$ giving a restriction of $\Delta t \leq 0.458\Delta t_{FE}$. This is approximately 15% less than the limiting case $\theta_* = 1$ ($C_{LM} = 0.537$ for $\theta_* = 1$). We provide the scheme to fifteen decimal digits in Table 3.2 and remark that the $\theta_{15} = 0.7$ constraint was active for this scheme.

It is natural to compare this TVB(4,4) scheme against the fourth-order extrapolated BDF scheme (eBDF4)

$$
\begin{aligned}
w_n &= \frac{48}{25}w_{n-1} - \frac{36}{25}w_{n-2} + \frac{16}{25}w_{n-3} - \frac{3}{25}w_{n-4} \\
&\quad + \frac{48}{25}\Delta t F_{n-1} - \frac{72}{25}\Delta t F_{n-2} + \frac{48}{25}\Delta t F_{n-3} - \frac{12}{25}\Delta t F_{n-4}\,.
\end{aligned}
$$
(3.5)

Since the nonlinear time-stepping restriction of eBDF4 is given by $C_{LM} = 7/32$, the new scheme provides for a 109% improvement in allowable (stable) step size over the best reported scheme (eBDF4) in [6]. Once again, the stability region of new scheme includes part of the imaginary axis and it compares favourably against that of the eBDF4 scheme; c.f. Figure 3.1.

TABLE 3.2
The coefficients of the numerically optimal four-step, fourth-order linear multistep scheme.

TVB(4,4)	a_i	b_i	C_{LM}
$i = 1$	2.628241000683208	1.618795874276609	0.458583744721242
$i = 2$	-2.777506277494861	-3.052866947601049	
$i = 3$	1.494730011212510	2.229909318681302	
$i = 4$	-0.345464734400857	-0.620278703629274	

3.4.2. Five-Step Schemes. If we consider five-step schemes, then it is possible to find fourth-order schemes that can be rewritten in an extended form that allows arbitrary starting values. For example, optimizing C_{LM} over the class of five-step, fourth-order linear multistep schemes with fifteen nonzero θ-values yields the $\text{TVB}_0(5,4)$ scheme presented in Table 3.3. This scheme satisfies the boundedness property (1.6) with $M \geq 1$ provided $\Delta t \leq 0.45\Delta t_{FE}$. Since $\theta_{16} = 0$, this scheme can be rewritten as a twenty-step scheme with non-negative coefficients. The stability region of $\text{TVB}_0(5,4)$ includes part of the imaginary axis and essentially coincides with TVB(4,4). See Figure 3.1.

By increasing the number of nonzero θ-values, we can obtain slightly larger C_{LM}-values. For example, optimizations using thirty θ-values produced a scheme with $C_{LM} = 0.471$. We do not reproduce that scheme here as it had similar behaviour in numerical tests to $\text{TVB}_0(5,4)$.

TABLE 3.3
The coefficients of the numerically optimal five-step, fourth-order linear multistep scheme.

$\text{TVB}_0(5,4)$	a_i	b_i	C_{LM}
$i = 1$	3.089334754787739	1.629978886421390	0.450202335599730
$i = 2$	-3.997727108450201	-3.839438825282836	
$i = 3$	2.799704082644115	3.698752623531085	
$i = 4$	-1.069321620028803	-1.688757722449064	
$i = 5$	0.178009891047150	0.305220798719644	

3.5. An Order-Five Scheme. We next study five-step, fifth-order linear multistep methods. For optimizing C_{LM} over this class we used twenty-five θ-values. This yields a scheme with $M \geq 1$ provided $\Delta t \leq 0.377 \Delta t_{FE}$. The coefficients of this optimal scheme are given in Table 3.4. This scheme has $\theta_{21} = 0$ which implies that it can be rewritten as a twenty-five step scheme that is monotone with arbitrary starting values.

As a basis for comparison, we consider the fifth-order extrapolated BDF scheme (eBDF5), which is given by

$$
(3.6) \quad \begin{aligned}
w_n &= \frac{300}{137} w_{n-1} - \frac{300}{137} w_{n-2} + \frac{200}{137} w_{n-3} - \frac{75}{137} w_{n-4} + \frac{12}{137} w_{n-5} \\
&+ \frac{300}{137} \Delta t F_{n-1} - \frac{600}{137} \Delta t F_{n-2} + \frac{600}{137} \Delta t F_{n-3} - \frac{300}{137} \Delta t F_{n-4} + \frac{60}{137} \Delta t F_{n-5} \,.
\end{aligned}
$$

The nonlinear time-stepping restriction of eBDF5 is $\Delta t \leq 0.0867 \Delta t_{FE}$ so $\text{TVB}_0(5,5)$ gives a 335% improvement in allowable (stable) step size over this extrapolated BDF scheme. The linear stability of the scheme is also favourable when compared against eBDF5; see Figure 3.2. However, we know the scheme cannot include the imaginary axis near the origin since it is impossible for any five-step, fifth-order scheme to do so [8]. On the other hand, it is seen that the boundary of the stability region stays very close to a segment of the imaginary axis and the corresponding maximal amplification factors on the imaginary axis are very close to 1. Because optimizations using $k = 6, 7$ gave similar time-stepping restrictions (the C_{LM}-values were 0.379 and 0.395, respectively) and did not produce a stricter linear stability near the origin we focus our attention on the five-step scheme, $\text{TVB}_0(5,5)$.

TABLE 3.4
The coefficients of the numerically optimal five-step, fifth-order linear multistep scheme.

$\text{TVB}_0(5,5)$	a_i	b_i	C_{LM}
$i = 1$	3.308891758551210	1.747442076919292	0.377052834833475
$i = 2$	-4.653490937946655	-4.630745565661800	
$i = 3$	3.571762873789854	5.086056171401077	
$i = 4$	-1.504199914126327	-2.691494591660196	
$i = 5$	0.277036219731918	0.574321855183372	

3.6. Sixth-Order Schemes.

3.6.1. Six-Step Schemes. The results for the sixth-order extrapolated BDF method (eBDF6) are less favourable than for lower-order eBDF schemes.

THEOREM 3.1. *For the eBDF6 scheme no positive C_{LM} value in (3.3) exists.*

Proof. To show that we cannot have $C_{LM} > 0$, note that the first step of the reformulation (3.1) for eBDF6 will give

$$
w_n = \left(\frac{360}{147} - \theta\right) w_{n-1} + \frac{360}{147} \Delta t F_{n-1} + \left(\frac{360}{147}\theta - \frac{15}{2}\right) w_{n-2} + \left(\frac{360}{147}\theta - \frac{720}{147}\right) \Delta t F_{n-2} + \cdots
$$

with $\theta = \theta_1$. It is impossible for both $\left(\frac{360}{147} - \theta\right)$ and $\left(\frac{360}{147}\theta - \frac{720}{147}\right)$ to be positive; hence the scheme does not possess a positive threshold value C_{LM}. □

Rewriting the general class of six-step methods of order six, using additional steps, we were unable to find extended schemes that allow for monotonicity with arbitrary starting values. Taking twenty-five distinct θ-values and $\theta_j = \theta_*$ for all $j \geq j_* = 25$
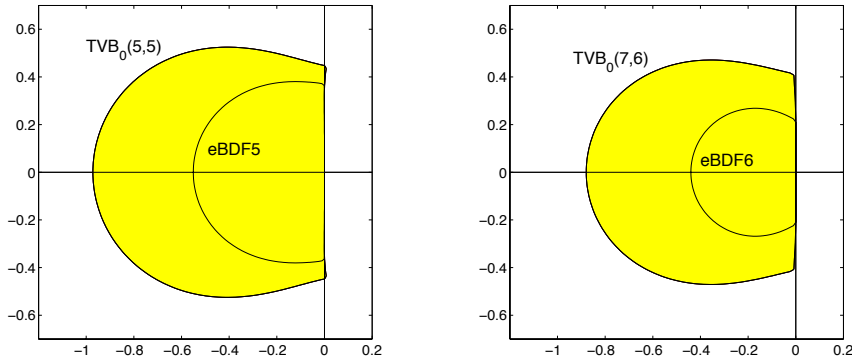
Fig. 3.2. *Stability regions for the eBDF5 and $TVB_0(5,5)$ schemes (left plot) and the eBDF6 and $TVB_0(7,6)$ schemes (right plot). The TVB(6,6) region is not plotted since it closely agrees with the $TVB_0(7,6)$ region.*

we found that C_{LM} increases as $\theta_* \in [0,1)$ increases. Based on a variety of numerical tests, it was found that the choice $\theta_* = 0.75$ gives a relatively large $C_{LM} = 0.328$ and moderate error constant, while adequately minimizing the possibility of oscillations arising from the startup procedures. See Table 3.5 for the coefficients of this scheme and Figure 3.2 for the linear stability region. Similar to the fifth-order case, the stability region of the TVB(6,6) scheme does not contain a segment of the imaginary axis near the origin, but its boundary is for a large part very close to the imaginary axis.

TABLE 3.5
The coefficients of the numerically optimal six-step, sixth-order linear multistep scheme.

TVB(6,6)	a_i	b_i	C_{LM}
$i = 1$	4.113382628475685	1.825457674048542	0.328491643359885
$i = 2$	-7.345730559324184	-6.414174588309508	
$i = 3$	7.393648314992094	9.591671249204753	
$i = 4$	-4.455158576186636	-7.583521888026967	
$i = 5$	1.523638279938299	3.147082225022105	
$i = 6$	-0.229780087895259	-0.544771649561925	

3.6.2. Seven-Step Schemes. If we consider seven-step schemes, then it is possible to find schemes of order six that can be rewritten as a scheme with larger step number and non-negative coefficients, giving monotonicity for arbitrary starting values.

Optimization of C_{LM} over the class of seven-step, sixth-order linear multistep schemes with twenty-five nonzero θ-values yields the $TVB_0(7,6)$ scheme presented in Table 3.6. This scheme satisfies the boundedness property (1.6) with $M \geq 1$ provided $\Delta t \leq 0.309\Delta t_{FE}$. Since $\theta_{26} = 0$, this scheme can be rewritten as an 32-step scheme with non-negative coefficients. The stability region of $TVB_0(7,6)$ essentially coincides with TVB(6,6) and does not contain a segment of the imaginary axis near the origin. The stability region is displayed in Figure 3.2.

4. Numerical Illustrations. In this section, we examine the numerical behaviour of our new TVD and TVB linear multistep methods and compare with

TABLE 3.6
The coefficients of the numerically optimal seven-step, sixth-order linear multistep scheme.

TVB$_0$(7,6)	a_i	b_i	C_{LM}
$i = 1$	4.611532883607545	1.861015137800509	0.309253747416378
$i = 2$	-9.451321766751356	-7.511070082780818	
$i = 3$	11.294453144657830	13.266237470507250	
$i = 4$	-8.568419982721693	-13.059962115416270	
$i = 5$	4.138363606421970	7.520216192319446	
$i = 6$	-1.174917528050790	-2.389309837695513	
$i = 7$	0.150309642836489	0.325922452117498	

more classical TVD schemes, mentioned in § 2, and some optimal TVD Runge-Kutta schemes, denoted as RK(s, p) where s is the number of stages and p the order. Our focus here is to illustrate the monotonicity and stability behaviour of the schemes rather than to provide a detailed accuracy study. If a study of the temporal accuracy was desired it would be more appropriate to consider systems with smooth solutions where the spatial discretization errors are dominated by the time stepping errors.

4.1. Linear Monotonicity Test. As a first, simple test we consider the maximum principle for the linear advection problem

$$u_t + u_x = 0$$

on spatial interval $0 \leq x \leq 1$, with inflow boundary condition $u(0, t) = 0$ and initial step function $u(x, 0) = 1$ on $(0, 1/2]$ and 0 elsewhere. The semi-discrete system in $\mathbb{R}^m$ is obtained by first-order upwind discretization in space with constant mesh width $\Delta x = 1/m$. For the test $m = 100$ is taken.

The PDE solution satisfies the maximum principle $0 \leq u(x, t) \leq 1$ and the same holds for the semi-discrete system. This property will be examined for the fully discrete solutions. The maximum principle could be replaced equivalently by max-norm monotonicity by considering an equivalent advection problem with $v(x, t) = 2u(x, t) - 1$.

Starting values for the multistep schemes were computed by the forward Euler method (FE) and the classical fourth-order Runge-Kutta method (RK4). Note that for this simple linear problem the classical Runge-Kutta method is monotone. For actual applications, a natural choice would be to use a monotone starting scheme of order $p-1$ or p for a multistep scheme of order p, in combination with a suitable spatial discretization. For this monotonicity test, using the first-order upwind discretization, only the choices FE and RK4 were considered for convenience.

Subsequently, the largest Courant numbers $\nu = \Delta t/\Delta x \in \{0.01, 0.02, \ldots\}$ were determined such that

$$-\epsilon \leq w_n \leq 1 + \epsilon \qquad \text{for} \quad n = 1, 2, \ldots, 1000,$$

with inequalities for the vectors $w_n \in \mathbb{R}^m$ component-wise. Of course, if $\epsilon = 0$ this is a genuine maximum principle. In exact arithmetic we could take $\epsilon = 0$ for a monotone scheme with rational coefficients. To cater for round-off and the fact that our schemes are not genuinely monotone we took as standard value $\epsilon = 10^{-15}$. However for the TVB(4,4) scheme ϵ-values larger than this default value were needed; those results were obtained with $\epsilon = 10^{-12}$. In the following tables the maximal Courant numbers are listed for the most interesting optimal schemes. For comparison, also the entries for the eBDF-schemes are presented.

TABLE 4.1
Linear monotonicity test: Maximal Courant numbers for the optimal k-step methods, $k = 3, 4$. The results for TVB(4,4) were obtained with $\epsilon = 10^{-12}$; this is indicated by the entries[(*)].

	eBDF3	TVD$_+$(3,2)	TVB$_0$(3,3)	eBDF4	TVD$_+$(4,3)	TVB(4,4)
C_{LM}	0.39	0.50	0.53	0.22	0.33	0.45
Exper.(FE)	0.41	0.50	0.53	0.26	0.34	0.46[(*)]
Exper.(RK4)	0.43	0.50	0.53	0.30	0.35	0.51[(*)]

TABLE 4.2
Linear monotonicity test: Maximal Courant numbers for the optimal k-step methods, $k = 5, 6, 7$.

	eBDF5	TVB$_0$(5,5)	TVB$_0$(5,4)	eBDF6	TVB(6,6)	TVB$_0$(7,6)
C_{LM}	0.08	0.37	0.45	0.00	0.32	0.30
Exper.(FE)	0.17	0.37	0.47	–	0.32	0.32
Exper.(RK4)	0.21	0.38	0.50	–	0.37	0.34

4.2. Nonlinear Test : Burgers' Equation. To further investigate the behavior of our time-stepping schemes, we consider one of Laney's five test problems [11], the evolution of a square wave by Burgers' equation

$$\frac{\partial u}{\partial t} + \frac{\partial}{\partial x}\left(\frac{1}{2}u^2\right) = 0$$

on the spatial interval $-1 \leq x \leq 1$ with periodic boundary conditions. In this test case, the discontinuous initial conditions

$$u(x,0) = \begin{cases} 1 & \text{for } |x| < 1/3, \\ -1 & \text{for } 1/3 < |x| \leq 1, \end{cases}$$

are evolved to time $t = 0.3$ using a constant grid spacing of $\Delta x = 1/320$. In this example, the jump at at $x = 1/3$ remains a steady shock and the jump at $x = -1/3$ creates a simple centered expansion fan between $c_1 = -1/3 - t$ and $c_2 = -1/3 + t$. Until the shock and expansion fan intersect, at time $t = 2/3$, the exact solution is [11]

$$u(x,t) = \begin{cases} -1 + 2\frac{x-c_1}{c_2-c_1} & \text{for } c_1 < x < c_2, \\ 1 & \text{for } c_2 < x < 1/3, \\ -1 & \text{elsewhere.} \end{cases}$$

The example is particularly interesting because it illustrates the behaviors near sonic points $(u = 0)$ that correspond to an expansion fan and a compressive shock.

Similar to [20, 15], we choose the finite-difference Shu-Osher schemes (ENO-type) for spatial discretization of the equation. These discretizations are derived using flux reconstruction and have a variety of desirable properties. For example, they naturally extend to an arbitrary order of accuracy in space, and they are independent of the time discretization, thus allowing experimentation with different time discretization methods. Moreover, educational codes are also freely available [11, 12], an attribute which is desirable for standardizing numerical studies. In our simulations we take the spatial order of accuracy in Δx to be the same as the temporal order of accuracy p. Flux splitting is taken as in [20, 15]. For further details on the underlying discretization as well as a code for the spatial discretization, see [11, 12].

4.2.1. Third-Order Experiments. To quantify the accuracy of the computed solution, we use the logarithm of the discrete L_1 errors at time $t_n = 0.3$

$$\log_{10} \Big(\frac{1}{m} \sum_{i=1}^{m} |w_i^n - u(x_i, t_n)| \Big),$$

where m is the number of grid points and w_i^n is the fully discrete solution in grid point x_i at time t_n. A plot of the error for a selection of third-order methods is given in Figure 4.1. To ensure a fair comparison for methods with a different number of function evaluations, the error is plotted as a function of the *effective CFL number*, $\Delta t/(s\Delta x)$ for a method taking s function evaluations per step, rather than the CFL number itself. This implies that for a particular plot, the total number of function evaluations at a particular abscissa value will be the same for each scheme. We started the computations with an effective CFL number of 0.02 and continued until the numerical scheme produced overflow (complete instability).

In this test example, we compare a number of three-step, third-order linear multistep schemes and the optimal three-stage, third-order TVD Runge-Kutta method RK(3,3) [9, 20]. All the multistep schemes are started using the RK(3,3) scheme. Of the schemes considered, the best performance is given by the new $TVB_0(3,3)$ scheme and the poorest performance is given by the classical TVD multistep scheme $TVD_{\pm}(3,3)$. In particular, the $TVB_0(3,3)$ scheme allows a 284% increase in the effective time step over $TVD_{\pm}(3,3)$ and 22% increase over the popular RK(3,3) scheme. The extrapolated BDF scheme also performs well, providing a 15% increase in the effective timestep over RK(3,3).

The oscillations in the error plots suggest that oscillations in the solutions arise for large enough time steps (and before the methods produce overflow). An examination of the total variation (TV) of the solutions verifies this conjecture and also leads us
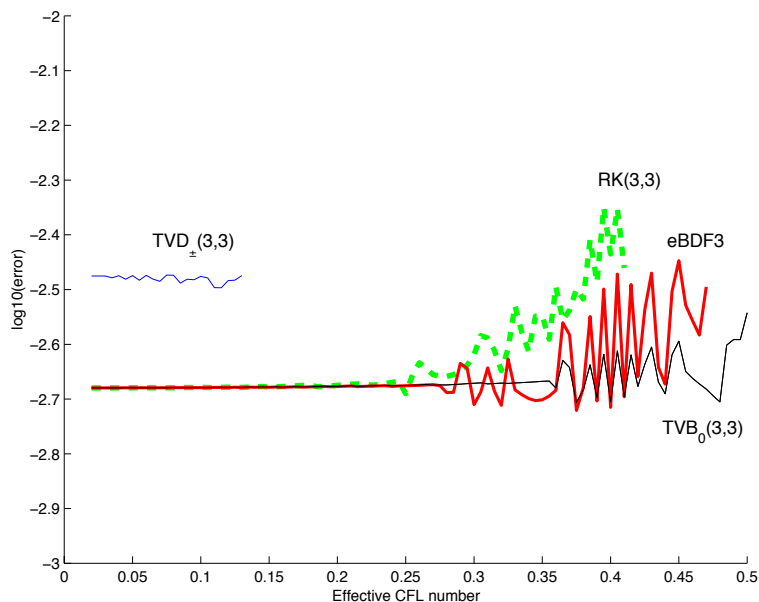

FIG. 4.1. *Burgers' equation: L_1 errors as a function of the effective CFL number for selected third-order schemes.*

to recommend the new TVB_0(3,3) scheme. In particular, we remark that the TV-increase for TVB_0(3,3) remains *very* small (less than 10^{-12}) up to an effective CFL number of 0.375. This represents an improvement in the time step-size of 213%, 25%, and 23% over the $\text{TVD}_{\pm}$(3,3), eBDF3, and RK(3,3) schemes, respectively.

Numerical experiments for the TVD_{+}(4,3) were also carried out. Use of this scheme is not generally recommended, however, because it requires more steps than the other multistep schemes under consideration and because it was found to develop oscillations and complete instability for smaller effective CFL numbers than any of RK(3,3), eBDF3 and TVB_0(3,3).

4.2.2. Fourth-Order Experiments. For a selection of fourth-order schemes the L_1 errors as a function of the effective CFL number are plotted in Figure 4.2. All the multistep schemes are started using the optimal TVD RK(5,4) scheme [9, 20]. We remark that the TVB(4,4) scheme gave similar results to TVB_0(5,4), so its plot is omitted for clarity. The TVD_{+}(5,4) scheme was also tested, but its plot is not included since its stability is not competitive with $\text{TVD}_{\pm}$(4,4).

Of the schemes considered here, the best performance is given by the new scheme TVB_0(5,4) and the weakest performance is given by the classical TVD multistep scheme $\text{TVD}_{\pm}$(4,4). More specifically, the TVB_0(5,4) scheme allows a 600% increase in the effective time step over $\text{TVD}_{\pm}$(4,4), a 13% increase over the RK(5,4) scheme, and a 2% increase over TVB(4,4). The extrapolated BDF scheme is not competitive with either RK(5,4) or TVB_0(5,4), although its performance is much better than $\text{TVD}_{\pm}$(4,4).

Our TVB_0(5,4) and TVB(4,4) results develop oscillations, but these remain small (i.e., the final TV-increase is always less than 5×10^{-9} for TVB(4,4) and 2×10^{-10} for TVB_0(5,4)) provided the effective CFL number is less than 0.34. The RK(5,4) scheme gives a negligible increase in the total variation (i.e., less than 3×10^{-15}) until an effective CFL number of 0.325, at which point it also exceeds 10^{-8}.

In most applications the small, bounded oscillations produced by TVB_0(5,4) and TVB(4,4) should be quite acceptable. However, fifth- and higher-order schemes produce larger oscillations. The source of these oscillations receives some attention in the next subsection.

4.2.3. Higher-Order Experiments. The L_1 errors as a function of the effective CFL number are plotted for a selection of fifth-order schemes in Figure 4.3. Our tests include the new TVB_0(5,5) scheme and the eBDF5 scheme. As a basis for comparison, we also include a recent nine-stage, fifth-order TVD Runge-Kutta method [15] that utilizes both upwind- and downwind- biased operators. For theoretical purposes, results for the twenty-five step TVD extension of the TVB_0(5,5) scheme are also included. Since fifth-order TVD Runge-Kutta methods must use downwind-biased discretizations [9, 16], we have taken a fourth-order TVD Runge-Kutta scheme, RK(5,4), as the startup procedure for all fifth-order multistep methods.

In this test we find a complete loss of stability for TVB_0(5,5) at an effective CFL number of about 0.35, which about 15% larger than RK(9,5) and 56% larger than eBDF5.

Surprisingly, the errors for TVB_0(5,5) are noticeably larger than for the extended scheme $\text{TVD}_{\text{ext}}(25,5)$, in particular for small CFL numbers. This is because the TVB_0(5,5) scheme, in combination with the fifth-order ENO discretization, generates some oscillations (the TV-increase averages 0.015 for effective CFL numbers less than 0.335) whereas the $\text{TVD}_{\text{ext}}(25,5)$ scheme does not (the TV-increase there always remains less than 3×10^{-15} for effective CFL numbers less than 0.335). We are
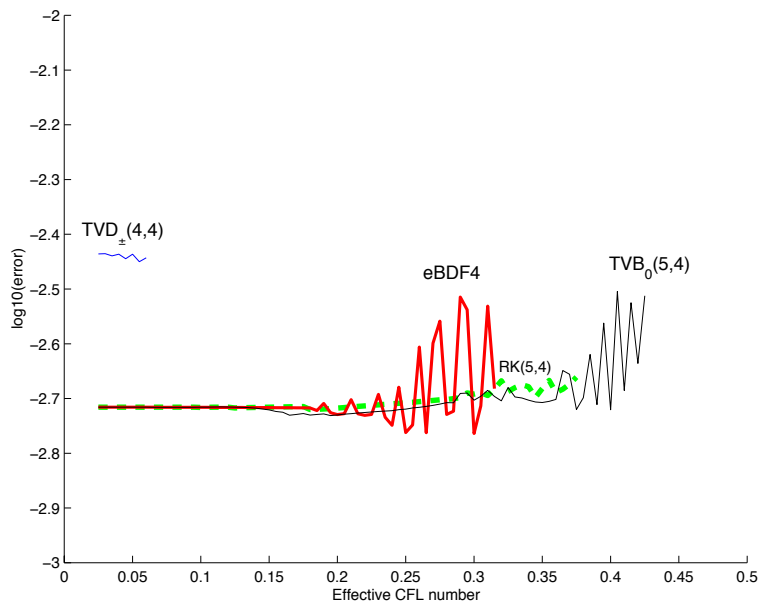
FIG. 4.2. *Burgers' equation: L_1 errors as a function of the effective CFL number for selected fourth-order schemes.*

investigating the source of this numerical behaviour. As a part of this work, we are considering improved startup procedures and methods which combine good linear and nonlinear stability. Our hope is to derive simple, efficient, high-order schemes which more strictly preserve the total-variation-diminishing property.

Tests for sixth-order schemes on this Burgers problem were also carried out. The overall conclusions were quite similar to those for fifth-order: the new $TVB_0(7,6)$ and $TVB(6,6)$ gave the largest steps before producing overflow. However, in combination with sixth-order ENO discretizations, both schemes produced oscillations. Also the extension of $TVB_0(7,6)$ to a TVD scheme with step number thirty-two showed quite large errors (larger than for the lower-order results in the previous figures) so here it seems that the combination of very high-order time stepping with the ENO discretizations is not entirely successful. Modifications and other spatial discretizations are currently under study.

5. Summary and Conclusions. In this paper new multistep methods are constructed that satisfy the TVB property with optimal step size restrictions. For several cases this actually leads to methods that are TVD in an extended sense: there is an equivalent multistep method, with larger step number, that is TVD with arbitrary starting values. In general, the size of the constant M in (1.6) will depend on the starting procedure.

Our theoretical and numerical studies show the superiority of these new methods over the classical TVD multistep schemes with non-negative coefficients of [18, 13, 2]. The new multistep methods are also more efficient in our tests than the optimal TVD (or SSP) Runge-Kutta schemes of [9, 15, 20].

In particular the third- and fourth-order schemes $TVB_0(3,3)$, $TVB(4,4)$ and $TVB_0(5,4)$ gave very clear and good results. For these methods a substantial gain may be expected in situations where both monotonicity and high accuracy are sought.
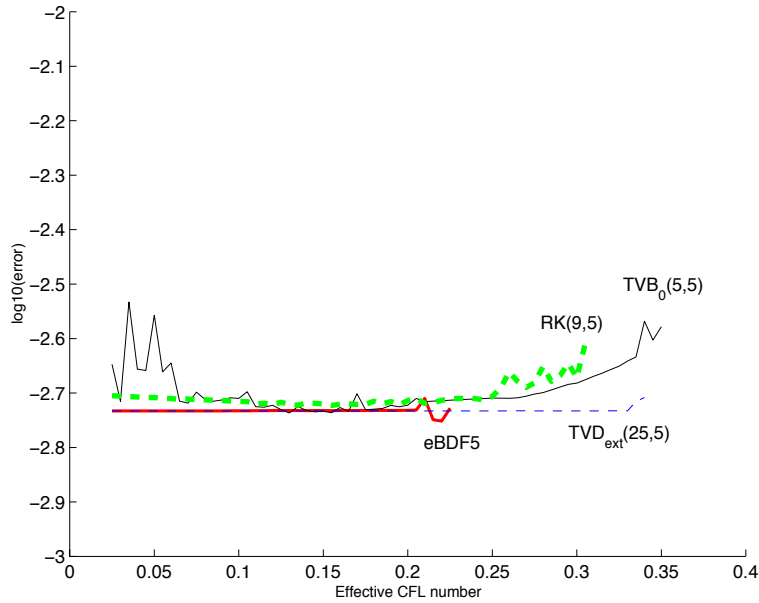
FIG. 4.3. *Burgers' equation: L_1 errors as a function of the effective CFL number for selected fifth-order schemes.*

For fifth- and sixth- order, theoretically optimal schemes were derived that performed very well on a linear monotonicity test. We also found that the combination of the $\text{TVB}_0(5,5)$ with a fifth-order ENO spatial discretization gave good stability on a Burgers' equation example, but with some visible oscillations. Since sixth-order schemes showed this behaviour in an even more pronounced way, we continue to study fifth- and sixth- order *combinations* of spatial discretization and time stepping that are appropriate for hyperbolic conservation laws.

For many applications an order of accuracy up to four will be sufficient, and then the new TVB multistep methods are recommended in combination with the ENO discretizations. These schemes produce accurate results that are essentially free of oscillations.

Appendix A. Tables of optimal monotone schemes for arbitrary starting values. In this appendix optimal monotone schemes with non-negative coefficients are listed for number of steps up to six and order three and four. Also optimal schemes with non-negative a_j and some $b_j < 0$ are listed for number of steps up to six and order up to six, complementing and improving some of the entries in [2]. See § 2 for a discussion.

Appendix B. The proof of Theorem 2.1. The conditions on the coefficients for having order 2 are

$$\sum_{j=0}^{k-1} a_{k-j} = 1 \quad \text{and} \quad \sum_{j=0}^{k-1} \left(j^q a_{k-j} + q\, j^{q-1} b_{k-j} \right) = k^q, \quad q = 1, 2\,.$$

Let $\sigma_j = \text{sgn}(b_j)$ and $c_j = a_j - K|b_j|$ with $K = \tilde{K}_{LM}$. Note that all $c_j \geq 0$. In terms

of these coefficients, the order conditions can also be written as

$$\sum_{j=0}^{k-1} \left(c_{k-j} + K|b_{k-j}| \right) = 1,$$

$$\sum_{j=0}^{k-1} \left(j\, c_{k-j} + (Kj + \sigma_{k-j})|b_{k-j}| \right) = k,$$

$$\sum_{j=0}^{k-1} \left(j^2 c_{k-j} + (Kj^2 + 2\sigma_{k-j}j)|b_{k-j}| \right) = k^2.$$

By taking a linear combination of these relations, it is easily seen that

$$\sum_{j=0}^{k-1} \left(k + (k-1)j - j^2 \right) c_{k-j} = -\sum_{j=0}^{k-1} \left(K(k + (k-1)j - j^2) - \sigma_{k-j}(1 - k + 2j) \right) |b_{k-j}|.$$

All terms in the sum of the left-hand side are non-negative. Hence, at least one of the terms in the sum of the right-hand side has to be non-positive. Since $\sigma_{k-j} = \pm 1$, it follows that

$$K \le \left| \frac{1 - k + 2j}{k + (k-1)j - j^2} \right|$$

for some index $0 \le j \le k - 1$. The maximum value is $(k-1)/k$, obtained with $j = 0$, $k - 1$.

REFERENCES

[1] M. TAWARMALANI AND N.V. SAHINIDIS, *Convexification and Global Optimization in Continuous and Mixed-Integer Nonlinear Programming: Theory, Algorithms, Software, and Applications.* Nonconvex Optimization and Its Applications 65, Kluwer, 2002.

[2] S. GOTTLIEB, C.-W. SHU AND E. TADMOR, *Strong stability preserving high-order time discretization methods.* SIAM Review 42 (2001), pp. 89-112.

[3] A. HARTEN, *On a class of high resolution total-variation-stable finite difference schemes*, SIAM J. Numer. Anal. 21 (1984), pp. 1-23.

[4] E. HAIRER, S.P. NØRSETT AND G. WANNER, *Solving Ordinary Differential Equations I – Non-stiff Problems.* Second edition, Springer Series in Comput. Math. 8, Springer, 1993.

[5] W. HUNDSDORFER AND S.J. RUUTH, *On Monotonicity and Boundedness Properties of Linear Multistep Methods.* In preparation.

[6] W. HUNDSDORFER, S.J. RUUTH AND R.J. SPITERI, *Monotonicity-preserving linear multistep methods.* SIAM J. Numer. Anal. 41 (2003), pp. 605-623.

[7] W. HUNDSDORFER AND J.G. VERWER, *Numerical Solution of Time-Dependent Advection-Diffusion-Reaction Equations.* Springer Series in Comput. Math. 33, Springer, 2003.

[8] R. JELTSCH AND O. NEVANLINNA, *Stability of explicit time discretizations for solving initial value problems.* Numer. Math. 37 (1981), pp. 61-91.

[9] J.F.B.M. KRAAIJEVANGER, *Contractivity of Runge-Kutta methods.* BIT 31 (1991), 482–528.

[10] J.D. LAMBERT, *Numerical Methods for Ordinary Differential Equations, the Initial Value Problem.* John Wiley & Sons, 1991.

[11] C.B. LANEY, *Computational Gasdynamics.* Cambridge University Press, 1998.

[12] C.B. LANEY, *CFD Recipes: Software for Computational Gasdynamics.* Web Address: http://capella.colorado.edu/~laney/booksoft.htm.

[13] H.W.J. LENFERINK, *Contractivity preserving explicit linear multistep methods.* Numer. Math. 55 (1989), pp. 213-223.

[14] R.J. LEVEQUE, *Finite Volume Methods for Hyperbolic Problems.* Cambridge Texts in Applied Mathematics, Cambridge University Press, 2002.

[15] S.J. RUUTH AND R.J. SPITERI, *High-order strong-stability-preserving Runge-Kutta methods with downwind-biased spatial discretizations.* To appear SIAM J. Numer. Anal.

[16] S.J. RUUTH AND R.J. SPITERI, *Two barriers on Strong-Stability-Preserving Time Discretization Methods.* J. Sci. Comput. 17 (2002), pp. 211-220

[17] S.J. RUUTH, *Global Optimization of Strong-Stability-Preserving Runge-Kutta schemes.* Submitted.

[18] C.-W. SHU, *Total-variation-diminishing time discretizations.* SIAM J. Sci. Stat. Comp. 9 (1988), pp. 1073-1084.

[19] C.-W. SHU AND S. OSHER, *Efficient implementation of essentially non-oscillatory shock-capturing schemes.* J. Comput. Phys. 77 (1988), pp. 439-471.

[20] R.J. SPITERI AND S.J. RUUTH, *A new class of optimal high-order strong-stability-preserving time-stepping schemes.* SIAM J. Numer. Anal. 40 (2002), pp. 469–491.

TABLE A.1
The coefficients of the optimal monotone multistep schemes $TVD_+(k,p)$ with non-negative coefficients and arbitrary starting values.

		$i=1$	$i=2$	$i=3$	$i=4$	$i=5$	$i=6$
$TVD_+(4,3)$	a_i	16/27	0	0	11/27		
$K_{LM}=1/3$	b_i	16/9	0	0	1/9		
$TVD_+(5,3)$	a_i	25/32	0	0	0	7/32	
$K_{LM}=1/2$	b_i	25/16	0	0	0	5/16	
$TVD_+(6,3)$	a_i	0.850708871672521	0.000000000000000	0.000000000000000	0.000000000000000	0.030664864534524	0.118626263792955
$K_{LM}=0.582822$	b_i	1.459638436015361	0.000000000000000	0.000000000000000	0.000000000000000	0.052614491749418	0.203537849338091
$TVD_+(5,4)$	a_i	0.048963857415660	0.000000000000000	0.008344481263515	0.043224046622448	0.899467614698377	
$K_{LM}=0.021190$	b_i	2.310657177903865	0.000000000000000	0.393785059936681	2.039789323347605	0.000000000000000	
$TVD_+(6,4)$	a_i	0.342460855717073	0.000000000000000	0.000000000000000	0.191798259434853	0.093562124938684	0.372178759909390
$K_{LM}=0.164759$	b_i	2.078553105578000	0.000000000000000	0.000000000000000	1.164112222279297	0.567871749748949	0.000000000000000

TABLE A.2
The coefficients of the optimal monotone multistep schemes $TVD_\pm(k,p)$ with downwinding and arbitrary starting values.

		$i = 1$	$i = 2$	$i = 3$	$i = 4$	$i = 5$	$i = 6$
TVD$\pm$(3,3)	a_i	0.5946107119086603	0.2808069515504443	0.1245823365402954			
$\tilde{K}_{LM} = 0.286532$	b_i	2.0751970086596670	-0.9800189169117666	0.4347935328844448			
TVD$\pm$(4,3)	a_i	0.7039668831130313	0.0000000000000000	0.1370262938463393	0.1590068750232294		
$\tilde{K}_{LM} = 0.414573$	b_i	1.6980533848146665	0.0000000000000000	-0.3305240414536602	0.3835438690401605		
TVD$\pm$(5,3)	a_i	0.7984934160506617	0.0000000000000000	0.0000000000000000	0.0444908636199906	0.1570157198737477	
$\tilde{K}_{LM} = 0.517173$	b_i	1.5439585769873690	0.0000000000000000	0.0000000000000000	-0.0860270718123650	0.3036039651786210	
TVD$\pm$(6,3)	a_i	0.8507088716725210	0.0000000000000000	0.0000000000000000	0.0000000000000000	0.0306648645345240	0.1186262637929550
$\tilde{K}_{LM} = 0.582822$	b_i	1.4596384360153610	0.0000000000000000	0.0000000000000000	0.0000000000000000	0.0526144491749418	0.2035378493380910
TVD$\pm$(4,4)	a_i	0.3978013074888790	0.2893736299849810	0.2584633583433857	0.0543617041822830		
$\tilde{K}_{LM} = 0.158694$	b_i	2.5067218697606790	-1.8234711479316890	1.6286918637394930	-0.3425571263489400		
TVD$\pm$(5,4)	a_i	0.5138252914465321	0.1754202755745120	0.0000000000000000	0.2439525892903640	0.0668012204991950	
$\tilde{K}_{LM} = 0.237094$	b_i	2.1671816335817790	-0.7398762675261580	0.0000000000000000	1.0289274170305640	-0.2817498574731950	
TVD$\pm$(6,4)	a_i	0.5367949436979945	0.0000000000000000	0.0000000000000000	0.0628170267627820	0.3084669771614380	0.0919210523778350
$\tilde{K}_{LM} = 0.283199$	b_i	1.8954694612116700	0.0000000000000000	0.0000000000000000	0.2218123647974770	1.0892236260161010	-0.3245812012019740
TVD$\pm$(5,5)	a_i	0.2500917149557949	0.2557101823576260	0.3259392832588550	0.1386456809409620	0.0296131038845850	
$\tilde{K}_{LM} = 0.086523$	b_i	2.8904519517036330	-2.9553873607256940	3.7670684358973900	-1.6024066358780370	0.3422554085470420	
TVD$\pm$(6,5)	a_i	0.3538847087653940	0.3020078111773320	0.2663131809195500	0.0000000000000000	0.0556260129916430	0.0221682861460810
$\tilde{K}_{LM} = 0.131335$	b_i	2.6945123889452290	-2.2995166748629710	2.0277343087983280	0.0000000000000000	-0.4235418412891150	0.1687914741219410
TVD$\pm$(6,6)	a_i	0.1496492007312780	0.2027269991349100	0.3271896010466640	0.2149388387623870	0.0910118354827690	0.0144835248419920
$\tilde{K}_{LM} = 0.046182$	b_i	3.2404070621153820	-4.3897194002264290	7.0847521316654590	-4.6541466820077150	1.9707114571514620	-0.3136168850417220